Breast Cancer Research and Treatment (2020) 182:9–19
https://doi.org/10.1007/s10549-020-05672-9

PRECLINICAL STUDY

Lipid biosignature of breast cancer tissues by matrix-assisted laser desorption/ionization time-of-flight mass spectrometry

Catarina L. Silva[1] · Rosa Perestrelo[1] · Ivo Sousa-Ferreira[2] · Filipa Capelinha[3] · José S. Câmara[1,4] · Marijana Petković[1]

Received: 4 January 2020 / Accepted: 6 May 2020 / Published online: 15 May 2020
© Springer Science+Business Media, LLC, part of Springer Nature 2020

Abstract

Purpose One of the hallmarks of cancer cells is the demand of supply for the synthesis of new membranes involved in cell proliferation and lipids have an important role in cellular structure, signaling pathways and progression of cancer. In this sense, lipid studies have become an essential tool allowing the establishment of signatures associated with breast cancer (BC). In this regard, some metabolic processes including proteins, nucleic acids and lipid synthesis are enhanced as part of cancer-associated metabolic reprogramming, as a requirement for cell growth and proliferation.

Methods Pairwise samples of breast active carcinoma (BAC) and breast cancer-free tissues were collected from $n = 28$ patients and analyzed by MALDI-TOF MS.

Results Major lipid species are identified in the MALDI-TOF mass spectra, with certain phosphatidylinositols (PIs) detectable only in BAC. Statistical analysis revealed significant differences ($p < 0.05$) between ratios lysophosphatidylcholine (LPC) 16:0/phosphatidylcholine (PC) 16:0_18:2 between AC and CF groups as well as for BC stages II and III. The ratio PC 16:0_18:2/PC16:0_18:1 was statistically different between AC and CF groups. The *one-way* ANOVA revealed that there are no statistical differences among BC stages (I, II and III) within AC group. Comparing BC stages, the significance impact increased ($p < 0.05$) with stage.

Conclusion The obtained data revealed MALDI-TOF MS as a powerful tool to explore lipid signatures and the enzyme activity associated with BC and possibly establish novel disease markers.

Keywords Breast cancer · Tissue · Lipids · Glycerophosphocholine · MALDI-TOF MS

Introduction

Breast cancer (BC) is leading at the top of women's diseases accounting expected to reach around 3 million of diagnosed cases by 2040, according to GLOBOCAN series of the International Agency for Research on Cancer (IARC) [1]. Available diagnostic and screening tools have supported the disease detection/progression resulting in the improved survival rates. Metabolomics emerged as a promising approach in disease profiling for the pursuit of new biomarkers in biological matrices, such as cell extracts, tissues or biological fluids, which reflect the altered metabolism and the physiological status [2]. Several techniques have been applied to biological samples (urine, exhaled breath, tissue) to explore the possible mechanisms underlying cancer, covering many classes of metabolites, namely intermediates of tricarboxylic acid cycle (TCA), amino acids and lipids. The most common

Electronic supplementary material The online version of this article (https://doi.org/10.1007/s10549-020-05672-9) contains supplementary material, which is available to authorized users.

✉ Marijana Petković
marijana.petkovic@staff.uma.pt

1 CQM - Centro de Química da Madeira, Universidade da Madeira, Campus Universitário da Penteada, 9020-105 Funchal, Portugal

2 Centro de Estatística e Aplicações, Faculdade de Ciências, Universidade de Lisboa, 1749-016 Lisboa, Portugal

3 Serviço de Anatomia Patológica, SESARAM, EPE. Hospital Dr. Nélio Mendonça, Avenida Luís de Camões, no 57–9004-514, Funchal, Portugal

4 Faculdade de Ciências Exactas e Engenharia da, Universidade da Madeira, Campus Universitário da Penteada, 9020-105 Funchal, Portugal

techniques include gas chromatography (GC), liquid chromatography (LC), tandem mass spectrometry (MS), nuclear magnetic resonance (NMR) spectroscopy and matrix-assisted laser desorption/ionization time-of-flight mass spectrometry (MALDI-TOF MS). In this regard, MALDI has gained popularity focusing on the global composition of lipids and their derivatives in biological systems becoming useful to search possible biomarkers for detection and prognosis of diseases [3, 4]. Lipids have an important role in cellular structure, signaling pathways and progression of cancer, being one of the hallmarks of cancer, the demand of energy and "constituents" supply for the synthesis of new membranes involved in cell proliferation [5–7]. They are divided into several subclasses—fatty acids, glycerophospholipids, sterols, sphingolipids, and others [8]. The advances in the development of matrices for MALDI analysis enabled to access the lipid composition [9, 10]. Changes in the lipid/glycerophospholipid composition of certain tissues suggest changes also in the activity of specific enzymes involved in the lipid metabolism. Overexpression of these enzymes is documented in various cancer types [11–15] and only for certain types, the associated changes in the glycerophospholipid composition was demonstrated.

Several studies have been developed using MALDI in diverse diseases, as well as in BC. Kang et al. [16] performed a study where protein and lipid profiles allowed the distinction of BCs according to the intrinsic subtype. Namely, glycerophosphocholines are overexpressed in BC compared to luminal and HER2 subtypes. In addition, Cho et al. [5] have found differences in the content of triacylglycerols (TGs) in healthy and BC tissues, as well as certain changes in the PC profile of the BC lipid extracts using MALDI MS. Kim et al. [17] developed an analytical approach for the determination of ketone-containing metabolites in human BC cell lines (e.g., MCF-7 cell line) as they can reflect the clinical condition and pathogenic mechanisms. Another report by Phillips et al. [18] demonstrated that MALDI MS imaging (MALDI MSI) of peptides obtained from BC tissues of patients with triple-negative BC (TNBC) were useful to discover proteins with higher abundance in TNBC when compared with non-cancerous tissue and use them in disease prognosis.

The current work describes the screening of lipid content from tissues obtained from active carcinoma (AC) tissue and comparison with cancer-free tissue (CF) samples to identify signatures associated with BC. Data are processed using *one-way* ANOVA and significant differences among BC stages within AC group were found. The results presented herein provide more insights about BC progression and strongly imply the impairment of the glycerophosphocholine metabolism in cancer cell that can be potentially related to the activities of enzymes and help in the discovery of BC biomarkers.

Materials and methods

Reagents and samples

Phosphate buffer solution (PBS) was from Sigma-Aldrich (St. Louis, MO, USA), methanol (MeOH) and chloroform ($CHCl_3$) from Thermo Fisher Scientific (Waltham, Massachusetts, USA). Matrices, 9-aminoacridine (9-AA) and 2,5-dihydroxybenzoic acid (DHB) and solvents for MALDI-TOF MS were from Sigma-Aldrich (St. Louis, MO, USA).

Tissue samples were obtained at the Pathologic Anatomy Unit of Hospital Dr. Nélio Mendonça (Funchal, Portugal) according to Table 1. The research was approved by the Ethics Committee of Funchal Central Hospital Dr. Nélio Mendonça (Approval no. S.1708625/2017) and has been performed in accordance with the ethical standards as laid down in the 1964 Declaration of Helsinki and its later amendments or comparable ethical standards. All the participants were fully informed of the objectives of the study and signed the informed consent.

Pairwise samples of active carcinoma (AC) and cancer-free (CF) tissues were resected from 28 female patients diagnosed with breast cancer (age range 44–84 years, average 65). The CF tissue is collected outside the tumor margin. The tissues were immediately frozen in liquid nitrogen and stored at − 80 °C until extraction.

The resected BC tissues were classified using the tumor, node, and metastasis staging (TNM) approach which included five cases of stage IA, eight cases of stage IIA, seven cases of stage IIB, one case of stage IIIA, five cases

Table 1 List of collected tissue samples from BC female patients. Histological grades are assigned as described in Materials and Methods section

Samples	Active carcinoma tissue
Number (*n*)	28
Age (range, median)	(44–84, 65)
Histological grade	IA (5)
	IIA (8)
	IIB (7)
	IIIA (1)
	IIIB (5)
	IIIC (2)

of stage IIIB and two of stage IIIC. Briefly, BC has four stages, I, II III and IV. Stage I and II have subcategories A and B, while stage III can have A, B or C. The letters describe the size of the tumor and if the tumor has spread to the axillary lymph nodes or the lymph nodes near the breastbone.

Methods

Lipid extraction

Portions of 100 mg of intact frozen samples were transferred into glass vials and rinsed with 5 mL of a PBS solution to remove any blood residues from the samples; 5 mL of cooled MeOH and $CHCl_3$ were added and samples homogenized. The vials were placed at − 20 °C and were vortexed three times every 10 min, followed by centrifugation (4000×*g* for 15 min, 4 °C). The lower phase ($CHCl_3$) containing the lipid fraction was kept in − 20 °C until analysis by MALDI-TOF MS.

MALDI-TOF MS

After the extraction procedure, 0.5 µL of tissue extracts were applied on the polished stainless-steel target plate followed by the same volume of matrix (10 mg/mL of DHB in methanol, or 10 mg/mL of 9-AA in acetone). Each sample was applied in duplicate for two consecutive days, to check reproducibility of the method. Each spectrum represents a sum of 2000 individual laser shots at 200 Hz frequency, with laser intensity around 40% of the maximum (internal scale). Ions were detected in both positive and negative mode, with the reflector detector (detector voltage was kept at 1970 V), to increase mass resolution, and with a delayed time of 120 ns, to increase mass precision [19]. MALDI-TOF MS was done at an Autoflex maX device (Bruker, Bremen, Germany) equipped with the Smartbeam-II™ laser emitting at 355 nm. The instrument has an improved system for detection of fragments (LIFT™ ion optics for single scan TOF/TOF acceleration), enabling the fragmentation of ions, which was used to confirm the signal identity.

LPC/PC and PC/PC ratios

Signal-to-noise (S/N) ratio of signals corresponding to the proton adduct of LPC 16:0 (*m/z* 496.3) was divided by the S/N ratio of signals arising from the proton adducts of PC 16:0_18:2 (*m/z* 758.6) or PC 16:0_18:1 (*m/z* 760.6) from the same spectrum and the number was averaged for a duplicate. S/N ratios of signals of the proton adducts of PC 16:0_18:2 and PC 16:0_18:1 from the same spectra are compared and the numbers statistically analyzed. The S/N values were extracted from the spectra acquired with 9-AA [20, 21].

Statistical analysis

Statistical analysis was performed using the Statistical Package for Social Sciences (SPSS) software version 23.0 package for Windows (SPSS Inc., Chicago, IL, USA). A paired samples *t* test was performed to verify whether there was statistical evidence that the mean difference between AC and CF tissues is different from zero for the three ratios LPC 16:0/PC 16:0_18:2, LPC 16:0/PC 16:0_18:1 and PC/PC as described in the previous section. In addition, significant differences between BC stages (I, II and III) within AC group were assessed with a *one-way* analysis of variance (ANOVA).

Results and discussion

Altered regulation of lipid metabolism in breast cancer is documented and potential mechanisms that lead to changes in the lipid composition discussed in numerous reports [22]. The upregulation of enzymes involved in the lipid metabolism, such as lysophosphatidylcholine acyltransferase, LPCAT [11–13], as well as phospholipase A_2, PLA_2 [14, 15] was found associated with the renal, gastric and breast cancer progression. On the other hand, there are no studies that correlate the upregulation of the enzyme with its activity, but such study is important, because these two enzymes have the opposite activities: LPCAT synthesizes PC, and PLA_2 catalyzes the hydrolysis of this glycerophospholipid and the production of LPC. In the equilibrium state/healthy cells, activities of these two enzymes require to be synchronized, due to well-known detergent-like and signaling properties of LPC [23].

The number of cancers, if not all, are associated with changes in the lipid metabolism, as discussed in several reports [7, 24]. Apparently, changes in the regulation of lipid metabolism play a role in BC carcinogenesis, as recently shown by Sevinsky et *al*. [22], emphasizing the importance of the lipid/glycerophospholipid profiling of AC tissues. Methods for lipid analysis involve lipid extraction, followed by fractionation into individual lipid classes and analysis of the fatty acid composition [25], presenting several disadvantages as time consuming and expensive. Nevertheless, the

first information about potential changes in lipid metabolism in AC tissues was revealed a decades ago by described approach. Furthermore, more modern method that is much easier and more specific provides the information about the spatial distribution and the concentration of a potential biomarkers is the mass spectrometric imaging (MSI) [26, 27]. MSI is mostly based on MALDI technology, and appears to be more powerful, since combines the advantages of MALDI profiling, histochemistry, and has the possibility of fragmentation [27], but MALDI MSI instrumentation not available in most laboratories. Therefore, analysis of tissue lipid composition by MALDI-TOF MS can be applied as an alternative to MSI, still keeping the advantages of the performances in terms of the time for analysis, sensitivity, precision and the extent of information that can be drawn from a single spectrum [10].

The signal intensity and MALDI-TOF MS quality depend on the homogeneity of the distribution of matrix/analyte co-crystals [28], and on the presence and relative abundance of the easy-detectable species, such as PC and/or sphingomyelin (SM) [29, 30]. These two species bear a pre-formed positive charge on the choline headgroup, and their presence might lead to a suppression of ion species with close *m/z* ratios [29].

Another issue are the overlapping of signals in the region between *m/z* around 700–900, and their misinterpretation [29, 31], but this can be overcome. Because of the high content of PC in tissue extracts and the possibility of overlapping with other PL species, for more detailed analysis of the spectra of tissue extracts, previous separation of the mixture in their individual class, by thin layer chromatography [32] might be recommended. On the other hand, it has been already demonstrated that this method can be applied for profiling of the lipid extracts from the tissues and cells [10, 31], which is the most time saving approach and is used in our study.

One of the approaches to overcome the drawbacks is the analysis of the complex spectra in the negative ion mode, the application of different matrices [21], and the fragmentation of specific ions. To assure signal identity in the lipid mixture extracted from tissues, we have compared the MALDI spectra acquired with DHB and 9-AA in the positive, as well as in the negative ion mode, as well as the fragmentation of ions with potentially overlapping position.

Organic extracts of AC tissues and CF are analyzed by MALDI-TOF MS with two matrices, DHB and 9-AA. These two matrices were selected because of their properties and complementarity for MALDI-TOF MS analyses of phospholipids: 9-AA works better performance in the negative ion mode than DHB [21, 29], and the spectra of tissue

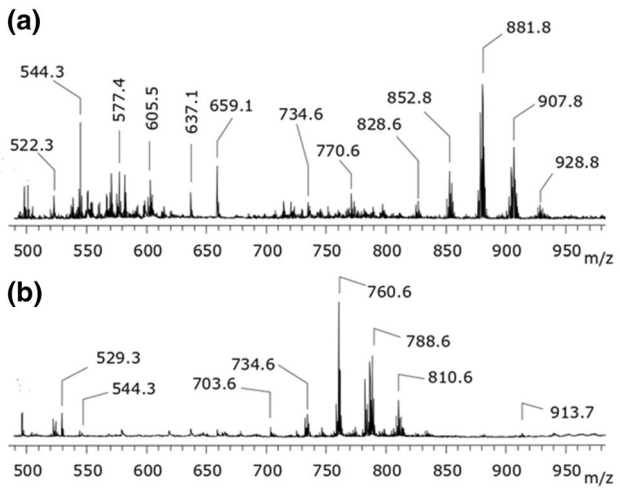

Fig. 1 Positive ion MALDI-TOF MS of tissue from a BC patient in stage IIA acquired with DHB (**a**) and 9-AA (**b**) matrix

extracts were different in terms of the detectable lipid species (Fig. 1a, b).

Positive ion mode spectra of BC extract acquired with DHB (Fig. 1b) contain a higher number of signals than the spectra acquired with 9-AA (Fig. 1a), which does not necessary indicate the higher number of detectable species. Both proton and the sodium adducts are favored with DHB with the intensity of adducts depending on the concentration of cations [33], whereas 9-AA favor the formation of proton adducts [21]. Moreover, under our conditions, triacylglycerols (TGs) were detectable mostly in the spectra acquired with DHB, and no changes in their fatty acid composition between AC and CF samples were found. TGs are, however, always detectable as the Na^+-adducts, what might be the reason of their favorable detection with DHB [34]. The position of the detected signals in the positive ion mode with both matrices and their identification is listed in Table 2.

The qualitative differences in the positive ion spectra of AC and CF tissues acquired with DHB were not found, and they will not be discussed further, and the corresponding negative ion mode spectra contain minor analyte signals, as described earlier [29, 31]. Therefore, for further analyses and discussion, the spectra acquired with 9-AA will be considered. We focus on the qualitative analyses, since quantitative analyses by MALDI are difficult, as detector response depends on a number of factors, such as *m/z* of the analyzed compounds [35].

Positive and negative MALDI-TOF MS of AC tissue extracts, and the corresponding CF tissue extracts are presented in Fig. 2a–d.

Table 2 Identification of signals detected in the positive ion mode MALDI-TOF mass spectra of BC and CF tissues

Signal position (*m/z*)	ion assignment
742–746	Fragments of PCs (Fuchs et al. [21].)
496.3	$[LPC\ 16:0+H]^+$
703.6	$[SM\ 16:0\_18:1+H]^+/[SM\ 16:1\_18:0+H]^+$
732.6	$[PE\ 16:0\_18:0+H]^+$
734.6	$[PC\ 16:0\_16:0+H]^+$
758.6	$[PC\ 16:0\_18:2+H]^+$
760.6	$[PC\ 16:0\_18:1+H]^+$
766.6	$[PC\ O\text{-}16:1\_\ 20:4+H]^+$ (O-alkyl PC, plasmalogen)
768.6	$[PC\ O\text{-}16:0\_20:4+H]^+$ (O-alkyl PC, plasmalogen)
770.6	$[PC\ 16:0\_\ 20:3+H]^+/[PC\ 18:1\_18:1+H]^+$
782.6	$([PC\ 36:4)+H]^+)/[PC\ 16:0\_20:4+H]^+/[PC\ 18:2\_18:2+H]^+$
784.6	$([PC\ 36:3)+H]^+)/[PC\ 18:1\_18:2+H]^+/[PC\ 16:0\_\ 20:3+H]^+$
786.6	$([PC\ 36:2)+H]^+)/[PC\ 18:0\_18:2+H]^+$
788.6	$([PC\ 36:1)+H]^+)/[PC\ 18:0\_18:1+H]^+$
808.6	$([PC\ 38:5)+H]^+)/[PC\ 18:1\_20:4+H]^+/[PC\ 18:2\_18:2+H]^+$
810.6	$([PC\ 38:4)+H]^+)/[PC\ 18:0\_20:4+H]^+$
828.8	$[PS\ 18:0\_18:1+K+H]^+/PS\ 16:0\_20:4\text{-}H+3Na]^+$
852	$[PS\ 18:0\_18:0+Na+K]^+$
881.8	$[TG\ 52:2+Na]^+$
885.5	$([PI\ 38:4)+H]^+)/[PI\ 18:1\_20:3+H]^+/[PC\ 16:0\_22:4+H]^+$
907.8	$[TG\ 54:3+Na]^+$
911.6	$([PI\ 40:6)+H]^+)/[PI\ 18:2\_22:4+H]^+$
913.6	$([PI\ 40:5)+H]^+)/[PI\ 18:1\_22:4+H]^{++}$
925.6	$([PI\ O\text{-}42:6)+H]^+)/[PI\ O\text{-}20:0\_22:6+H]^+$
928.8	$[PI\ 18:1\_20:4+2Na]^+$
939.6	$([PI\ 42:6)+H]^+)/[PI\ 20:0\_22:6+H]^+$
941.6	$([PI\ 42:5)+H]^+)/[PI\ 20:1\_22:4+H]^+$
951.7	$([PI\ 42:0)+H]^+)/[PI\ 20:0\_22:0+H]^+$
953.6	$([PI\ 43:6)+H]^+)/[PI\ 21:0\_22:6+H]^+$
955.5	$([PI\ 43:5)+H]^+)/[PI\ 21:0\_22:5+H]^+$
979.7	$([PI\ 44:0)+H]^+)/[PI\ 22:0\_22:0+H]^+$

Spectra were acquired with 9-AA and DHB in the reflector mode and delayed extraction conditions

Numbers represent the total number of carbon atoms and double bonds

LPC lysophosphatidylcholine, *PC* glycerophosphocholine, *PE* glycerophosphoethanolamine, *P I*glycerophosphoinositol, *SM* phosphosphingolipid, *TAG* triacylglycerol

The representative spectra of one selected tissue extract is presented in Fig. 2, whereas the selected spectra of patients operated in different BC stages are given in Fig. S1. It should be indicated that the detection of PIs, as negative ions that require two cations for charge compensation and ionization, in the positive ion mode spectra acquired with 9-AA was rather difficult, and the detectability of those ions and their composition is discussed later in the manuscript.

By the analysis of the PC region in the positive ion mode spectra acquired with 9-AA, there are differences in the intensities of the signal at *m/z* 758.6 related to the signal at 760.6 in AC versus non-cancerous tissues, namely in the extract of AC tissues, the signal at *m/z* 758.6 is lower when compared to the signal at 760.6 (Fig. 3).

Both arise from the proton adducts of PC, but one containing 18:2, and another 18:1 fatty acid residue at the *sn*-2 position (Table 2). To check for potential relation to the type of AC tissue and the stage, we have taken the ratio between the S/N of both signals. Since the S/N ratios differ significantly and MALDI is known for rather low shot-to-shot reproducibility [35], two S/N ratios were compare, as the measure of the ion concentration ratios between the

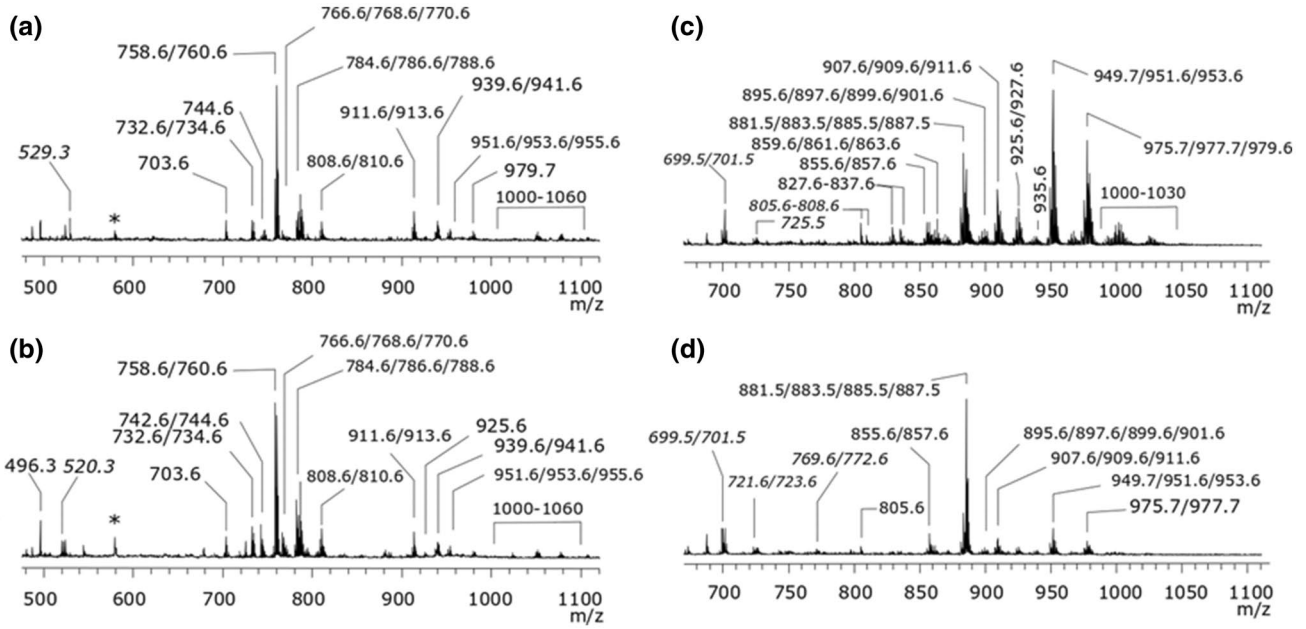

Fig. 2 Positive (**a**, **b**) and negative (**c**, **d**) MALDI-TOF MS of an AC tissue (stage IIA) (**a**, **c**) and the corresponding CF (**b**, **d**). Spectra were acquired with 9-AA as matrix and in the reflector mode under delayed extraction conditions. Signals are indicated according to their position (*m/z* ratio), whereas the signals arising from matrix are indicated by an asterisk

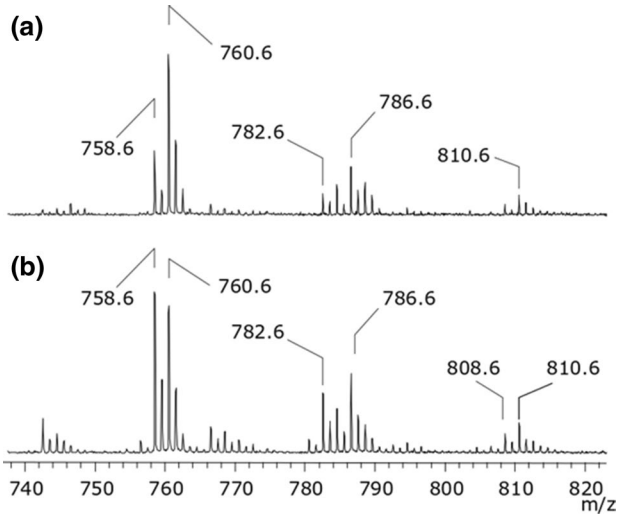

Fig. 3 Positive ion mode MALDI-TOF MS of the PC region from AC tissue (**a**) and the corresponding CF (**b**) acquired with 9-AA as matrix. Spectra were acquired in the reflector mode with delayed extraction conditions

samples. This approach overcomes the drawback of the MALDI methodology, as it has been shown for the organic extracts from serum of rheumatoid arthritis and Parkinson's disease patients [36, 37]. In addition to this, to check potential changes in the activity of the PLA_2, an enzyme that catalyzes the cleavage of the fatty acid from the *sn*-2 position of the lipid, the S/N ratio of the signal at *m/z* 496.3 (LPC 16:0) and both PCs at *m/z* 758.6 and *m/z* 760.6 were compared. Statistical analysis was performed, and the results of paired *t* tests are summarized in Table 3.

Firstly, the Kolmogorov–Smirnov test was performed to validate the normality assumption before performing a *t* test. Afterward, a paired *t* test was applied to the three ratios LPC 16:0/PC 16:0_18:2, LPC 16:0/PC 16:0_18:1 and PC 16:0_18:2/PC 16:0_18:1, considering all stages combined, as well as in separately for each BC stage I, II and III. Regarding to ratio LPC 16:0/PC 16:0_18:2 it could be verified that for all stages together there are statistically significant differences ($p < 0.05$) between AC and CF groups, as well as for the stages II and III. In addition, it can be also verified that within BC stages, the impact of significance augmented among the stages (0.393, 0.049 and 0.002), thus indicating that for advanced stages of the disease the lipid metabolism might be increasingly compromised. For the ratio LPC 16:0/PC 16:0_18:1, although there is no statistical evidence that the AC and CF are different, the same pattern observed in the previous ratio is viewed (0.833, 0.147 and 0.141). Concerning the ratio PC16:0_18:2/PC16:0_18:1 it was verified that for all stages together there are statistically significant differences between AC and CF groups, but the referred pattern is not expressed in this case.

Table 3 Summary of descriptive analysis, normality tests and paired *t* test for each ratio LPC/PC (*m/z* 758), LPC/PC (*m/z* 760) and PC/PC applied to active carcinoma (AC) and cancer-free (CF) tissue samples

	Ratio	Descriptive (mean ± SD)		K–S[a] (Normality)				Paired samples *t* test[b]			
		AC	CF	AC		CF		Mean	SD	Statistic	*p* value
				Statistic[c]	*p* value	Statistic	*p* value				
All stages together	LPC/PC (*m/z* 758)	0.503 ± 0.320	0.263 ± 0.142	0.127	0.200	0.096	0.200	0.240	0.334	3.810	7.29×10^{-4}
	LPC/PC (*m/z* 760)	0.250 ± 0.146	0.276 ± 0.166	0.124	0.200	0.140	0.170	− 0.025	0.218	− 0.618	0.542
	PC/PC	0.534 ± 0.236	1.059 ± 0.285	0.139	0.179	0.160	0.050	− 0.526	0.342	− 8.136	9.71×10^{-9}
Stage I	LPC/PC (*m/z* 758)	0.291 ± 0.359	0.143 ± 0.054	0.249	0.200	0.214	0.200	0.148	0.346	0.957	0.393
	LPC/PC (*m/z* 760)	0.148 ± 0.160	0.163 ± 0.071	0.291	0.194	0.272	0.200	− 0.015	0.154	− 0.023	0.833
	PC/PC	0.592 ± 0.183	1.121 ± 0.340	0.263	0.200	0.214	0.200	− 0.529	0.244	− 4.855	0.008
Stage II	LPC/PC (*m/z* 758)	0.519 ± 0.311	0.324 ± 0.143	0.149	0.200	0.119	0.200	0.196	0.365	2.141	0.049
	LPC/PC (*m/z* 760)	0.258 ± 0.135	0.347 ± 0.176	0.132	0.200	0.164	0.200	− 0.089	0.232	− 1.530	0.147
	PC/PC	0.505 ± 0.199	1.057 ± 0.229	0.156	0.200	0.188	0.134	− 0.552	0.287	− 7.690	1.00×10^{-6}
Stage III	LPC/PC (*m/z* 758)	0.617 ± 0.279	0.208 ± 0.112	0.188	0.200	0.150	0.200	0.409	0.206	5.253	0.002
	LPC/PC (*m/z* 760)	0.306 ± 0.144	0.194 ± 0.103	0.255	0.186	0.201	0.200	0.112	0.175	1.694	0.141
	PC/PC	0.558 ± 0.352	1.022 ± 0.389	0.211	0.200	0.238	0.200	− 0.464	0.524	− 2.343	0.058

[a]K–S—Kolmogorov–Smirnov (normality test) with Lilliefors correction;

[b]These values correspond to the paired differences AC–CF;

[c]Observed value related to K–S test regarding normality

Finally, for the AC group the *one-way* ANOVA was applied to compare the mean of each ratio among of the three independent BC stages I, II and III. For this purpose, the assumptions for adequately perform this statistical analysis was checked, namely each group sample is drawn from a normally distributed population (as shown in Table 3) and it can be assumed that there is a homogeneity of variances among populations (where for the ratios LPC 16:0/PC 16:0_18:2, LPC 16:0/PC 16:0_18:1 and PC 16:0_18:2/PC16:0_18:1 the *p* values of the Levene test were 0.821, 0.940 and 0.325, respectively). The *one-way* ANOVA revealed that there are no significant differences among the BC stages, regardless of the ratio considered (where for the ratios LPC 16:0/PC 16:0_18:2, LPC 16:0/PC 16:0_18:1 and PC16:0_18:2/PC16:0_18:1 the *p* values of the *F* test were 0.213, 0.173 and 0.750, respectively). This might indicate that for the collected sample the mean of each ratio is not affected by the disease stage.

Similar study that will connect the overexpression of enzymes with their activity with the stage of AC has not yet been performed. Our results indicate significant differences between AC and CF regarding the relative content of PCs with different fatty acid composition, but the differences are no significant among various stages of BC. Even if the LPCAT is upregulated in breast cancer [12] and LPCAT activity is enhanced in BC cells, its seems that it does not correlate with the cancer stage, at least judging by the PC/PC ratio (Table 3). On the other hand, certain specificity of the LPCAT toward incorporation of less unsaturated fatty acid into PC can be implied.

Additionally, the relative content of LPC, most likely the product of PC hydrolyzes catalyzed by PLA_2 is higher in AC compared to CF, and we found a correlation of LPC/PC (16:0_ 18:2) ratio with the cancer stage. These results imply that the activity of PLA_2 can be increasing with the stage of breast cancer [38, 39], but since there are several types of PLA_2 in the cells it remains to be clarified, which PLA_2 form is more active and it can be associated with the BC stage. It is, however, possible that factors other than BC stage can affect the activities of enzymes, but further study with more samples is required to better explore all involved factors.

Glycerophosphoinositols (PIs) are targeted as potential biomarkers for prostate cancers [26], as revealed by MSI, and their involvement in the signal transduction is demonstrated as reviewed by Kim et *al.* [40]. This is not surprising because, these negatively charged glycerophospholipids play an important role in the signal transduction [41, 42], the former one through the interaction and activation of some protein kinases, whereas the phosphorylation of PIs controls the membrane trafficking, which is the important process for the activation of various kinases. Simultaneously with the analysis of positive ions, the negative ion mode spectra were performed, once these ions are not easily detectable in positive ion mode; their signals are mostly suppressed by the easily detectable signals of neutral glycerophospholipids.

The negative ion mode spectra of AC and CF tissues are given in Fig. 4, and the corresponding signal assignment in Table 4. The negative ion mode MALDI-TOF mass spectra of other stages are given in Fig. S1.

The differences in the PI composition between the AC and CFs are reflected in the appearance of new PI species in the spectra of BC tissues, and the frequency of occurrence is given in Table 5.

In most AC, PI 16:0_18:1 is detectable (*m/z* 835.5), whereas this PI was not detectable in the CF. Besides this PI, PI 18:0_18:1 and 18:0_18:2 (at *m/z* 861.5 and 863.5, respectively) is detected in most AC tissues (Table 5). AC in stage I according to the composition of PIs is not clearly different compared to CF, whereas other PI species appear more frequently in other BC stages.

There are also some negatively charged ions at higher *m/z* ratios, which might correspond to phosphorylated glycerophosphoinositols, but their identity remains to be confirmed and data analyzed with a higher number of samples. These highly phosphorylated PIs are difficult for detection by MALDI MS, as demonstrated earlier [43]. Even if PIs were considered as potential markers for prostate and some other cancers [26, 44], it cannot be confirmed in this case for breast cancer and under applied experimental conditions.

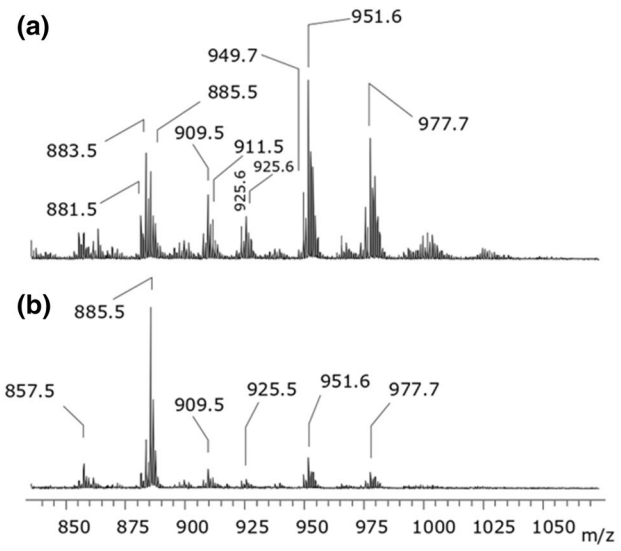

Fig. 4 Negative ion mode MALDI-TOF MS from AC tissue extract (**a**) and the corresponding surrounding CF tissue (**b**). Spectra were acquired with 9-AA as matrix, in the reflector mode with delayed extraction conditions

Table 4 Identification of signals detected in the negative ion mode MALDI-TOF MS of BC and CF tissues

Signal position (*m/z*)	Ion assignment
808.6	([PC 38:4)−H]$^-$)/[PC 18:0_20:4−H]$^-$
827.5	([PI 34:5)−H]$^-$)/[PI 16:1_18:4−H]$^-$
829.5	([PI 34:4)−H]$^-$)/[PI 16:0_18:4−H]$^-$
835.5	([PI 34:1)−H]$^-$)/[PI 16:0_18:1−H]$^-$
837.5	([PI 34:0)−H]$^-$)/[PI 16:0_18:0−H]$^-$
855.6	([PS 41:3)−H]$^-$)/[PS 20:3_21:0−H]$^-$
857.5	([PI 36:4)−H]$^-$)/[PI 16:0_20:4−H]$^-$
859.5	([PI 36:3)−H]$^-$)/[PI 18:1_18:2−H]$^-$
861.5	([PI 36:2)−H]$^-$)/[PI 18:0_18:2−H]$^-$
863.5	([PI 36:1)−H]$^-$)/[PI 18:0_18:1−H]$^-$
881.5	([PI 38:6)−H]$^-$)/[PI 16:0_22:6−H]$^-$
883.5	([PI 38:4)−H]$^-$)/[PI 16:0_22:4−H]$^-$/[PI 18:2_20:3−H]$^-$
885.5	([PI 38:3)−H]$^-$)/[PI 16:0_22:3−H]$^-$/[PI 18:1_20:3−H]$^-$
887.5	([PI 38:2)−H]$^-$)/[PI 16:0_22:2−H]$^-$/[PI 18:0_20:3−H]$^-$
895.6	([PI O−40:6)−H]$^-$)/[PI O−18:0_22:6−H]$^-$
897.6	([PI O−40:5)−H]$^-$)/[PI O−18:0,_22:5−H]$^-$
899.6	([PI O−40:4)−H]$^-$)/[PI O−18:0_22:4−H]$^-$
901.6	([PI O−40:3)−H]$^-$)/[PI O-18:0_22:3−H]$^-$
907.5	([PI 40:7)−H]$^-$)/[PI 18:0_20:3−H]$^-$
909.5	([PI 40:6)−H+]$^-$)/[PI 18:0_22:6−H]$^-$
911.6	([PI 40:5)−H]$^-$)/[PI 18:0_22:5−H]$^-$
925.6	([PI 41:5)−H]$^-$)/[PI 19:1_22:4−H]$^-$
927.6	([PI 41:4)−H]$^-$)/[PI 19:0_22:4−H]$^-$
935.6	([PI 41:0)−H]$^-$)/[PI 20:0_21:0−H]$^-$/[PI 22:0_19:0−H]$^-$
937.6	([PI 42:6)−H]$^-$)/[PI 20:0_22:6−H]$^-$
939.6	([PI 42:5)−H]$^-$)/[PI 20:1_22:4−H]$^-$
949.7	([PI 42:0)−H]$^-$)/[PI 20:0_22:0−H]$^-$
951.6	([PI 43:6)−H]$^-$)/[PI 21:0_22:6−H]$^-$
953.6	([PI 43:5)−H]$^-$)/[PI 21:0_22:5−H]$^-$
975.7	([PI 44:1)−H]$^-$)/[PI 22:0_22:1−H]
977.7	([PI 44:0)−H]$^-$)/[PI 22:0_22:0−H]$^-$
1000–1050	Signals in this region could arise from phosphatidylinositol phosphates, but their identification could not be confirmed with certainty

Spectra were acquired with 9-AA and in the reflector mode, and delayed extraction conditions

Numbers represent the total number of carbon atoms and double bonds

PC glycerophosphocholine, *PI* glycerophosphoinositol

Table 5 Occurrence of the glycerophosphoinositol species (PI) that appear in the AC tissue and not detectable in the surrounding CF tissue

Stage of cancer	Glycerophosphoinositol (m/z)	Frequency of occurrence (%)
I	No clear differences between AC and CF in PI region	
II	PI 16:0_18:1 (835.5)	77.7
	PI 18:0_18:1 (863.5)	77.
	PI 18:0_18:2 (861.5)	61.1
	PI 18:0_20:3 (907.5)	66.6
III	PI 16:0_18:1 (835.5)	30
	PI 18:0_18:1 (863.5)	30
	PI 18:0_20:3 (907.5)	60

Only the samples in which different PIs are detected are indicated

PI glycerophosphoinositol

Conclusions

In conclusion, in this study we have verified that LPC/PC ratio, calculated from MALDI mass spectra can be used as a marker for BC disease progression, and that the PC content is most likely affected by the changes in the PLA_2 activity, and that its activity increases with the AC stage. On the other hand, it seems that the activity of LPCAT remains not changed during the disease progression. The changes in the activity of enzymes involved in the PI metabolism could not be well documented, at least no by lipid profiling by MALDI-TOF MS.

Results present in this study emphasize the importance of the determination of the activity of enzymes involved in lipid metabolism apart from their expression, once the concentration of the products from their enzymatic activity does not correlate with their expression in BC tissue.

Acknowledgements This work was supported by *FCT-Fundação para a Ciência e a Tecnologia* (project PEstOE/QUI/UI0674/2019, CQM, UID/MAT/00006/2019, CEAUL, Portuguese Government funds, and INNOINDIGO/0001/2015), Madeira 14-20 Program (project PROEQUIPRAM—Reforço do Investimento em Equipamentos e Infraestruturas Científicas na RAM—M1420-01-0145-FEDER-000008) and by *ARDITI-Agência Regional para o Desenvolvimento da Investigação Tecnologia e Inovação* through the project M1420-01–0145-FEDER-000005—Centro de Química da Madeira—CQM + (Madeira 14-20).

Author contributions CS: conception of studies and experimental design, AC and CF tissue extractions, data analysis and manuscript preparation. RP: design of experiments and data analysis**.** IF: performed the statistical analysis and interpretation; FC: histological classification of AC tissues; JSC: manuscript preparation. MP: Performed the MALDI analyses, interpretation and manuscript preparation.

Compliance with ethical standards

Conflict of interest The authors declare that they have no conflict of interest.

Ethical approval Written informed consent was obtained from all patients prior to sample collection. The study protocol was approved by the Ethics Committee of Funchal Central Hospital Dr. Nélio Mendonça (Approval n. S.1708625/2017). This is also described in the "Methods" section.

References

1. Bray F, Ferlay J, Soerjomataram I et al (2018) Global cancer statistics 2018: GLOBOCAN estimates of incidence and mortality worldwide for 36 cancers in 185 countries. CA Cancer J Clin 68:394–424
2. Koek MM, Jellema RH, van der Greef J et al (2011) Quantitative metabolomics based on gas chromatography mass spectrometry: status and perspectives. Metabolomics 7:307–328
3. Jelonek K, Ros M, Pietrowska M, Widlak P (2013) Cancer biomarkers and mass spectrometry-based analyses of phospholipids in body fluids. Clin Lipidol 8:137–150
4. Cho YT, Su H, Chiang YY et al (2017) Fine needle aspiration combined with matrix-assisted laser desorption ionization time-of-flight/mass spectrometry to characterize lipid biomarkers for diagnosing accuracy of breast cancer. Clin Breast Cancer 17:373–381.e1
5. Cho YT, Su H, Huang TL et al (2013) Matrix-assisted laser desorption ionization/time-of-flight mass spectrometry for clinical diagnosis. Clin Chim Acta 415:266–275
6. Islam SR, Manna SK (2019) Lipidomic analysis of cancer cell and tumor tissues. Methods Mol Biol 1928:175–204
7. Long J, Zhang C-J, Zhu N et al (2018) Lipid metabolism and carcinogenesis, cancer development. Am J Cancer Res 8:778–791
8. Fahy E, Cotter D, Sud M, Subramaniam S (2011) Lipid classification, structures and tools. Biochim Biophys Acta 1811:637–647
9. Kim IC, Lee JH, Bang G et al (2013) Lipid profiles for HER2-positive breast cancer. Anticancer Res 33:2467–2472
10. Fuchs B, Schiller J (2008) MALDI-TOF MS analysis of lipids from cells, tissues and body fluids. Subcell Biochem 49:541–565
11. Du Y, Wang Q, Zhang X et al (2017) Lysophosphatidylcholine acyltransferase 1 upregulation and concomitant phospholipid alterations in clear cell renal cell carcinoma. J Exp Clin Cancer Res 36:66
12. Abdelzaher E, Mostafa MF (2015) Lysophosphatidylcholine acyltransferase 1 (LPCAT1) upregulation in breast carcinoma contributes to tumor progression and predicts early tumor recurrence. Tumor Biol 36:5473–5483
13. Uehara T, Kikuchi H, Miyazaki S et al (2016) Overexpression of lysophosphatidylcholine acyltransferase 1 and concomitant lipid alterations in gastric cancer. Ann Surg Oncol 23:206–213
14. Chen H-Z, Qu Y-H, Diao C-Y et al (2016) Expression of phospholipase A2 in breast cancer tissues and its significance. Int J Clin Exp Pathol 9(11):11820–11825
15. Yamashita SI, Yamashita JI, Ogawa M (1994) Overexpression of group II phospholipase A2 in human breast cancer tissues is closely associated with their malignant potency. Br J Cancer 69:1166–1170
16. Kang HS, Lee SC, Park YS et al (2011) Protein and lipid MALDI profiles classify breast cancers according to the intrinsic subtype. BMC Cancer 11:465

17. Kim KJ, Kim HJ, Park HG et al (2016) A MALDI-MS-based quantitative analytical method for endogenous estrone in human breast cancer cells. Sci Rep 6:1–7
18. Phillips L, Gill AJ, Baxter RC (2019) Novel prognostic markers in triple-negative breast cancer discovered by MALDI-mass spectrometry imaging. Front Oncol 9:379
19. Schiller J, Süß R, Arnhold J et al (2004) Matrix-assisted laser desorption and ionization time-of-flight (MALDI-TOF) mass spectrometry in lipid and phospholipid research. Prog Lipid Res 43:449–488
20. Leopold J, Popkova Y, Engel K, Schiller J (2018) Recent developments of useful MALDI matrices for the mass spectrometric characterization of lipids. Biomolecules 8:173
21. Fuchs B, Bischoff A, Sü R et al (2009) Phosphatidylcholines and -ethanolamines can be easily mistaken in phospholipid mixtures: a negative ion MALDI-TOF MS study with 9-aminoacridine as matrix and egg yolk as selected example. Anal Bioanal Chem 395:2479–2487
22. Sevinsky CJ, Khan F, Kokabee L et al (2018) NDRG1 regulates neutral lipid metabolism in breast cancer cells. Breast Cancer Res 20:55
23. Law S-H, Chan M-L, Marathe GK et al (2019) An updated review of lysophosphatidylcholine metabolism in human diseases. Int J Mol Sci 20:1149
24. Hao W, Friedman A (2014) The LDL-HDL profile determines the risk of atherosclerosis: a mathematical model. PLoS ONE 9:e90497
25. Punnonen K, Hietanen E, Auvinen O, Punnonen R (1989) Phospholipids and fatty acids in breast cancer tissue. J Cancer Res Clin Oncol 115:575–578
26. Goto T, Terada N, Inoue T et al (2014) The expression profile of phosphatidylinositol in high spatial resolution imaging mass spectrometry as a potential biomarker for prostate cancer. PLoS ONE 9:e90242
27. Sparvero LJ, Amoscato AA, Dixon CE et al (2012) Mapping of phospholipids by MALDI imaging (MALDI-MSI): realities and expectations. Chem Phys Lipids 165:545–562
28. Harvey DJ (1996) Matrix-assisted laser desorption/ionisation mass spectrometry of oligosaccharides and glycoconjugates. J Chromatogr A 720:429–446
29. Petković M, Schiller J, Müller M et al (2001) Detection of individual phospholipids in lipid mixtures by matrix-assisted laser desorption/ionization time-of-flight mass spectrometry: phosphatidylcholine prevents the detection of further species. Anal Biochem 289:202–216
30. Fuchs B, Süß R, Schiller J (2010) An update of MALDI-TOF mass spectrometry in lipid research. Prog Lipid Res 49:450–475
31. Petković M, Vocks A, Müller M et al (2005) Comparison of different procedures for the lipid extraction from HL-60 cells: A MALDI-TOF mass spectrometric study. Zeitschrift fur Naturforsch-Sect C J Biosci 60:143–151
32. Teuber K, Riemer T, Schiller J (2010) Thin-layer chromatography combined with MALDI-TOF-MS and 31P-NMR to study possible selective bindings of phospholipids to silica gel. Anal Bioanal Chem 398:2833–2842
33. Schiller J, Süß R, Fuchs B et al (2007) The suitability of different DHB isomers as matrices for the MALDI-TOF MS analysis of phospholipids: Which isomer for what purpose? Eur Biophys J 36:517–527
34. Schiller J, Süß R, Petković M, Arnold K (2002) Thermal stressing of unsaturated vegetable oils: Effects analysed by MALDI-TOF mass spectrometry,1H and31P NMR spectroscopy. Eur Food Res Technol 215:282–286
35. Schiller J, Arnhold J, Benard S et al (1999) Lipid analysis by matrix-assisted laser desorption and ionization mass spectrometry: a methodological approach. Anal Biochem 267:46–56
36. Angelini R, Vortmeier G, Corcelli A, Fuchs B (2014) A fast method for the determination of the PC/LPC ratio in intact serum by MALDI-TOF MS: An easy-to-follow lipid biomarker of inflammation. Chem Phys Lipids 183:169–175
37. Miletić Vukajlović J, Drakulić D, Pejić S et al (2019) Increased plasma phosphatidylcholine/lysophosphatidylcholine ratios in patients with Parkinson's disease. Rapid Commun Mass Spectrom 34:8595
38. Kamčeva T, Radisavljevič M, Vukičevič I, et al (2013) Interactions of platinum and ruthenium coordination complexes with pancreatic phospholipase A 2 and phospholipids investigated by MALDI TOF mass spectrometry. Chem Biodivers 10:1972–1986
39. Petković M, Müller J, Müller M et al (2002) Application of matrix-assisted laser desorption/ionization time-of-flight mass spectrometry for monitoring the digestion of phosphatidylcholine by pancreatic phospholipase A2. Anal Biochem 308:61–70
40. Kim Y, Shanta SR, Zhou LH, Kim KP (2010) Mass spectrometry based cellular phosphoinositides profiling and phospholipid analysis: A brief review. Exp Mol Med 42:1–11
41. Margaria JP, Ratto E, Gozzelino L et al (2019) Class II PI3Ks at the intersection between signal transduction and membrane trafficking. Biomolecules 9:104
42. Dogliotti G, Kullmann L, Dhumale P et al (2017) Membrane-binding and activation of LKB1 by phosphatidic acid is essential for development and tumour suppression. Nat Commun 8:1–2
43. Müller M, Schiller J, Petković M et al (2001) Limits for the detection of (poly-)phosphoinositides by matrix-assisted laser desorption and ionization time-of-flight mass spectrometry (MALDI-TOF MS). Chem Phys Lipids 110:151–164
44. Milne SB, Ivanova PT, DeCamp D et al (2005) A targeted mass spectrometric analysis of phosphatidylinositol phosphate species. J Lipid Res 46:1796–1802

Publisher's Note Springer Nature remains neutral with regard to jurisdictional claims in published maps and institutional affiliations.